International Journal of Nanoelectronics and Materials
Volume 13 (Special Issue) May 2020 [439-448]

Nanoscale Graphene Nanoparticles Conductive Ink Mechanical Performance Based on Nanoindentation Analysis

Hartini Saad[1,2], Mohd Azli Salim[2,3]*, Nor Azmmi Masripan[2], Adzni Md. Saad[2] and Feng Dai[4]

[1]*Jabatan Kejuruteraan, Sekolah Kejuruteraan dan Sains Kreatif, Kolej Yayasan Pelajaran Johor, Jalan Kulai – Kota Tinggi, KM 16, Jalan Kulai, 81000 Johor, Malaysia.*
[2]*Fakulti Kejuruteraan Mekanikal, Universiti Teknikal Malaysia Melaka, Hang Tuah Jaya, 76100 Durian Tunggal, Melaka, Malaysia.*
[3]*Advanced Manufacturing Centre, Universiti Teknikal Malaysia Melaka, Hang Tuah Jaya, 76100 Durian Tunggal, Melaka, Malaysia.*
[4]*China Railway Eryuan Engineering Group Co., Ltd, No. 3 Tongjin Road, Chengdu, China.*

ABSTRACT

Common conductive inks can be classified into three categories, which are noble metals, conductive polymers and carbon nanomaterials. Carbon nanomaterials offer many potential opportunities to be applied in printed and flexible electronics. Therefore, this paper aims to produce highly functional conductive ink using graphene nanoparticles with epoxy as a binder. As a baseline, graphene-filler conductive ink was formulated using a minimum percentage at the beginning. Then, the filler loading was increased based on the required conductivity level. This is to make sure the materials are in contact with each other and the movement of an electron will become easier. The formulation of ink, mixing process, printing process and curing process were performed to produce highly conductive graphene ink. The electrical and mechanical properties were assessed using a Four-point probe as per ASTM F390 and Dynamic Ultra Micro Hardness (DUMH) test as per ASTM E2546-1. Graphene Nanoplatelet (GNP) aggregates are unique nanoparticles consisting of shorts stacks of graphene sheets with platelets shape. They typically consist of aggregates of sub-micron platelets that have a particle diameter less than 2 microns, typical particle thickness of a few nanometers, a bulk density of 0.2 to 0.4 g/cc, an oxygen content of <2 wt%, the carbon content of >98 wt%, and in the form of black granules. In this paper, the effect on sheet resistivity and nanoindentation for straight line-shape, curve-shape, square-shape and zig-zag-shape circuits printed on Thermoplastic Polyurethane (TPU) substrate using Graphene Nanoparticles (GNPs) conductive ink as the connection material were investigated. The samples in this study were fabricated using a screen-printing method with a fixed circuit width of 1 mm, 2 mm and 3 mm. The straight-shape circuit, curve-shape, square-shape and zig-zag-shape circuits represent the electrical connection with 180°, A°, 90° and B° directional angles. The effect of varying circuit width on the sheet resistivity of all printed circuit mentioned before was later measured using Four-point probe. Nanoindentation was conducted using instrumental machines with indenter load and indenter displacement that can be continuously and simultaneously recorded during indenter loading and unloading.

Keywords: Conductive Ink, Graphene Nanoparticles, Sheet Resistivity.

1. INTRODUCTION

Conductive ink is composed of a conductive material, a thermoplastic polyvinylbutyral terpolymer binder, and a glycol ether solvent [1]. A conductive particulate having an average size from 0.5 to 10 microns and an aspect ratio of at least 3 to 1, such as silver flake can be used in this application. Conductive ink can be formulated by binding either nanoparticles or micro size particles that are highly conductive such as silver, copper, zinc, or carbon.

*Corresponding Author: *azli@utem.edu.my*

Conductive polymers are organic polymers that can offer high electrical conductivity and have been used in many applications, particularly in antistatic materials. They possess some limitations in terms of the manufacturing cost, material inconsistencies, toxicity, poor solubility in solvents, inability to directly undergo the melting process and their mechanical properties are not similar to other commercial polymers [2]. The conductive polymer composites are synthesized by adding conductive fillers such as carbon-based materials. It is because carbon-based materials have higher electrical conductivity than polymers and possess excellent mechanical properties. Therefore, graphene as a carbon-based material is chosen because of its lightweight, ability to form a conductive network easily and high in oxidation resistance [2].

Graphene is also known as a wonder material. It has been proven by the numerous research articles published in the same field [3]. These studies revealed the multi-functionality of the 2-D atomic crystal of graphene, which integrates the distinctive properties such as thermal conductivity (5000 $Wm^{-1}K^{-1}$) with high electron mobility at room temperature, high surface area per unit mass (2630 m^2 g^{-1}), high modulus of elasticity (1 TPa), and high electrical conductivity [4-8]. The graphene was used to make electronic devices for a variety of applications and graphene-based ink has been used to fabricate conductive components for a range of demonstrator applications in printed electronics using inkjet printing, gravure-printing, screen-printing, transfer-printing and 3D printing [9-16]. The inkjet, transfer, and gravure printing techniques offer high-resolution graphene patterns [16], but screen-printing is a practical option when low resistance is required. This is because screen-printing can produce thick films (µm range) in a single pass, reduce processing times and allow easy integration with the high-throughput manufacturing process.

For mechanical characterization of such printed samples, nanoindentation has been established as an important tool for submicron instrumented machines. Indenter load and indenter displacement can be continuously and simultaneously recorded during indenter loading and unloading [16]. The two mechanical properties most frequently measured are Young's modulus, E (GPa) and hardness, H (GPa). The unloading data are then analysed according to a model for the deformation of an elastic half-space by an elastic punch, which relates the contact area at peak load to the elastic modulus [17]. Methods for independently estimating the contact area from the indenter shape function are then used to provide separate measurements of E (GPa) and H (GPa) [17]. The elastic contact problem plays a key role in the analysis procedure by Boussinesq and Hertz. A method based on potential theory for computing stress and displacements in an elastic body loaded by a rigid, axisymmetric indenter was developed by Boussinesq. This method has subsequently been used to derive solutions for some important geometries such as cylindrical and conical indenters [17-19]. The significance of this study is to investigate the electrical and mechanical behaviours of different patterns using graphene nanoparticles conductive ink based on the nanoindentation analysis.

2. MATERIAL AND METHODS

2.1 Sample Preparation

2.1.1 Graphene Ink Preparation

The 0.7 g graphene nanoplatelets were mixed with 1.3 g BPA epoxy and 0.39 g hardener TETA to formulate the conductive ink. The binder was weighed on the analytical balance to obtain the gross weight. The weight of the mixture should be slightly higher than the desired value within the tolerance of ±0.05 g. An analytical balance was used to measure the mass of material. The beaker was put at the centre of the weighing pan and the door was shut. It was left behind for a few seconds for the unit to stabilize. In order to obtain accurate data when the substance was being weighed, the weight of the baker was waived out by pressing the tare button until the

display screen showed 0 g. Then, the door was opened and the materials were carefully put inside the beaker until the display exhibited the required weight according to the value of desired weight

2.1.2 Screen-Printing of Graphene Ink

The graphene conductive ink was used as the material and printed into four different test patterns. The test pattern 1 was a straight-line pattern, test pattern 2 was curve pattern, test pattern 3 was a square pattern and test pattern 4 was a zig-zag pattern. The entire pattern was designed with 15 cm × 4 cm of length and width of 1 mm, 2 mm and 3 mm. The sample preparation was started with cutting the TPU substrate with the dimension of 15 cm × 4 cm. Then, the TPU was placed at the back of the stencil using cellophane tape. After that, the conductive inks were spread over onto the back of the stencil. Finally, the TPU was then being taken off from the stencil.

2.1.3 Curing Process

The curing process is a post-treatment that was carried out after the printing of the conductive ink. The curing process is a chemical reaction in which the epoxide groups in epoxy resin reacts with hardener to form a highly cross-linked, three-dimensional network that provides high modulus and strength, good resistance to creep and good performance at elevated temperature [20-21]. The curing process is needed to improve the bonding between the particles of filler, binder and hardener. Curing is also applied with the purpose to melt the epoxy and to harden the mixture with the help of hardener thus, improving the adhesion between ink and the substrate. Curing process in this study took place at 100°C for 30 minutes inside universal oven UF55. By setting up the oven earlier, the printed sample placed on a tray can be put into the oven right after the printing process was completed. The purpose was to prevent the sample from being affected by external factors such as room temperature. After the printed sample was cured, it was then let to be fully dried at room temperature. After the curing process, the samples were ready to be analysed.

2.2 Sheet Resistivity

The sheet resistance of the conductive ink was determined using JANDEL In-Lane Four Point Probes with a 1 mm distance between each probe according to the ASTM F390 standard. In order to measure the resistance of cured ink, the probe was held in firm contact with the ink track. The four-point probe works by forcing the constant current along with the two outer probes and the voltage is read out from the two inner probes. About six data were recorded and the average resistivity was calculated. Based on the ASTM standard, the value of sheet resistance depends on the geometry of the sample.

2.3 Nanoindentation

Nanoindentation analysis was carried out using Dynamic Ultra Micro Hardness (DUMH) test using a three-sided pyramidal (Berkovich) diamond tip. Berkovich indenter tip is ideal for most testing purposes. It induces plasticity at very small loads, which produces a meaningful measurement of hardness. The Berkovich indenter tip has a large included angle, which minimizes the influence of friction. The basic principle of the nanoindenter test is by employing a high-resolution actuator to force an indenter into the test surface and a high-resolution to continuously measure the resulting penetration. As the indenter is driven into the material, both elastic and plastic deformations cause the formation of a hardness impression in conforming to the shape of the indenter to some contact depth. After the indenter is withdrawn, only the elastic portion of the displacement is recovered and this recovery enables one to determine the elastic properties of the material. The first step of measurement was preparing a sample and mounting it on a sample stage. The evaluation of hardness and elastic modulus were according ASTM

E2546-15 standard. After placing the sample on the stage into the indenter, the height of the measuring sample must be adjusted to the fixed height of the referenced material. The height adjustment of the sample can be done with small thumbwheel at the sample holder. Finally, when samples were in line with referenced material, the measurement parameters could be set. All measurements were done at the same depth of indentation to avoid the possibility of perforation of the printed sample. The nanoindenter test was conducted to describe the elastic behaviour of the printed ink. The test method used was the Continuous Stiffness Method (CSM), which able to plot the curve of hardness and modulus by continuously varying the indentation depth. The five indentations had been made for each sample. Each sample was measured in five different positions. During each test run, a personal computer collected and stored data for the load and displacement as the indenter was driven into the sample. Then, the raw data was used to construct the load-displacement graph.

3. RESULTS AND DISCUSSION

3.1 Sheet Resistivity

Figures 1 to 4 show the sheet resistivity at different width for four different patterns. By referring to the figure, sheet resistivity increased by increasing the width of the samples from 1 mm width to 2 mm and for 3 mm width, sheet resistivity decreased slightly. The sheet resistivity of the zig-zag pattern also increased gradually when the width of the samples increased. The increase and decrease of the sheet resistivity depend on the nature of the material and the physical shape or pattern affects the resistance of the samples.

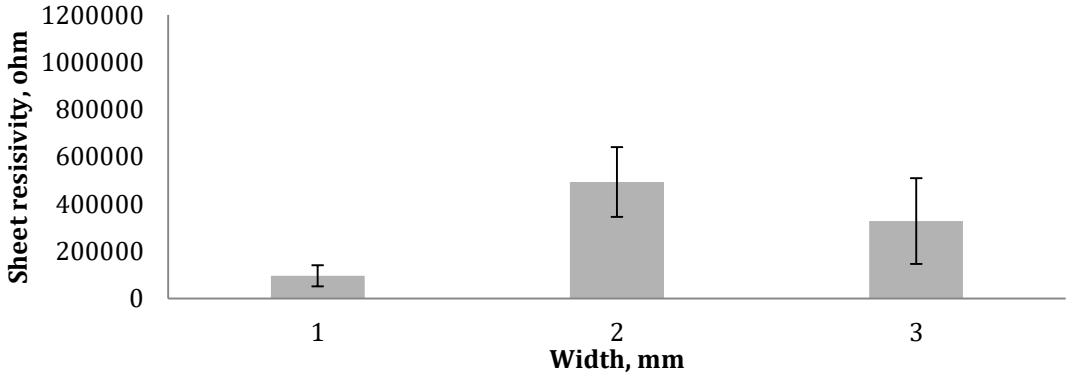

Figure 1. Sheet resistivity at different widths for the straight-line pattern.

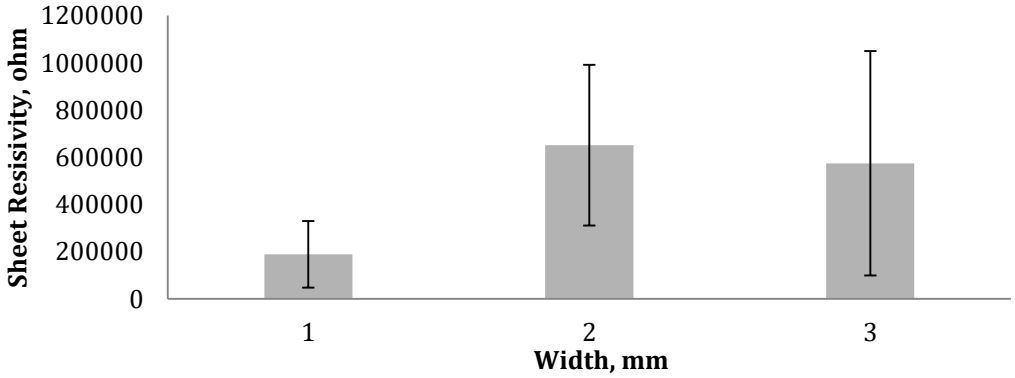

Figure 2. Sheet resistivity at different widths for the curve pattern.

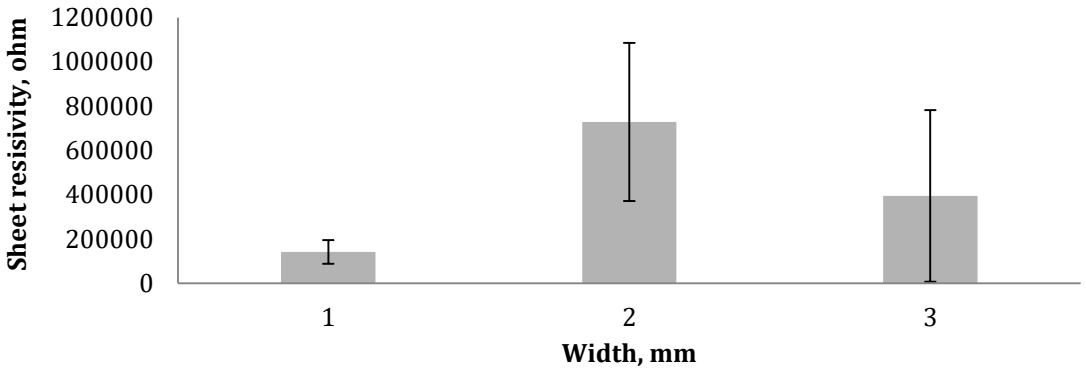

Figure 3. Sheet resistivity at different widths for the square pattern.

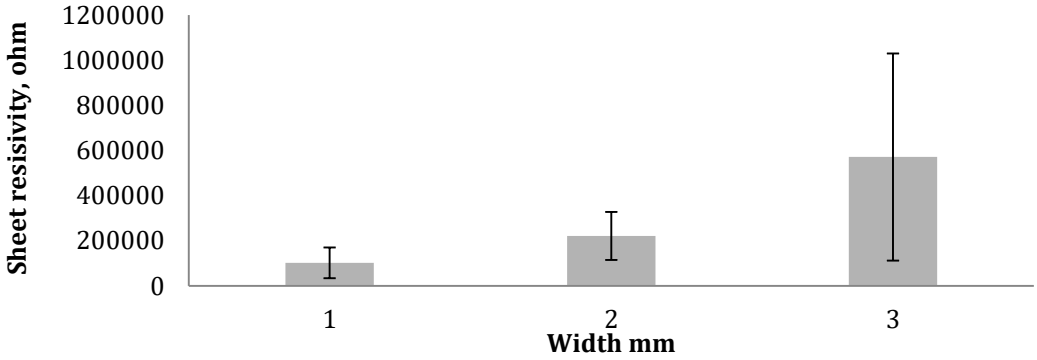

Figure 4. Sheet resistivity at different widths for the zig-zag pattern.

Then, Figures 5 to 7 show sheet resistivity at different patterns based on 1 mm width to 3 mm width. For 1 mm width, the sheet resistivity of curve pattern states the highest value of 189032.472Ω/sq., and the lowest values of sheet resistivity is for the straight line with 96342.286Ω/sq. For 2 mm width, the sheet resistivity of square pattern states the highest value of 728495.3Ω/sq., and the lowest values of sheet resistivity is a zig-zag pattern with 221211.3322Ω/sq. For 3 mm width, the sheet resistivity of zig-zag pattern states the highest value of 571495.975Ω/sq., and the lowest values of sheet resistivity is a straight line with 328242.879Ω/sq. According to the trend for zig-zag pattern, the smaller the width, the value of sheet resistivity decreases. If the width is bigger, the value of sheet resistivity values will increase. As a conclusion, in the printed samples of graphene ink with and without thermal effect, resistance is the opposition to the flow of electrons through the material in response to an applied voltage. Conductors have very small resistances and allow electrons to flow easily if a voltage is applied. Insulators have large resistance and do not allow electrons to flow easily.

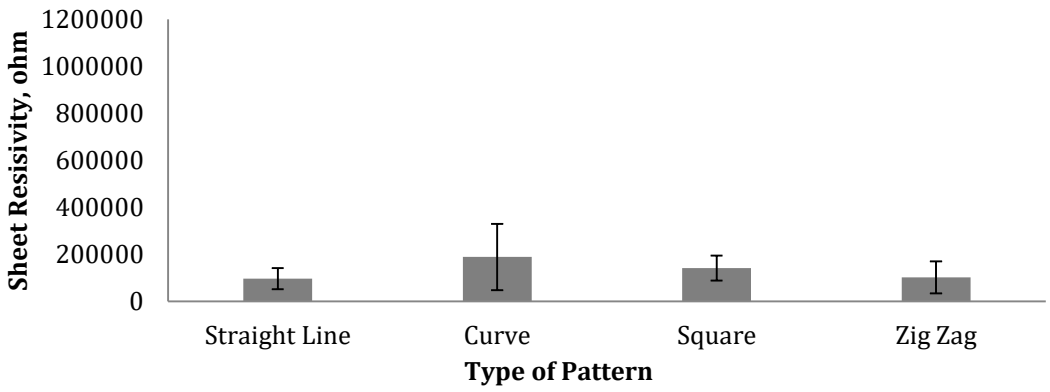

Figure 5. Sheet resistivity at different patterns for 1 mm width.

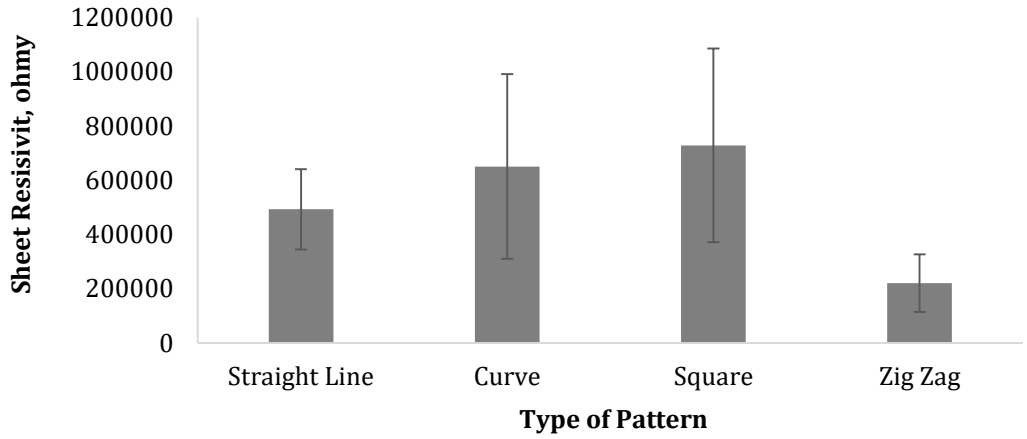

Figure 6. Sheet resistivity at different patterns for 2 mm width.

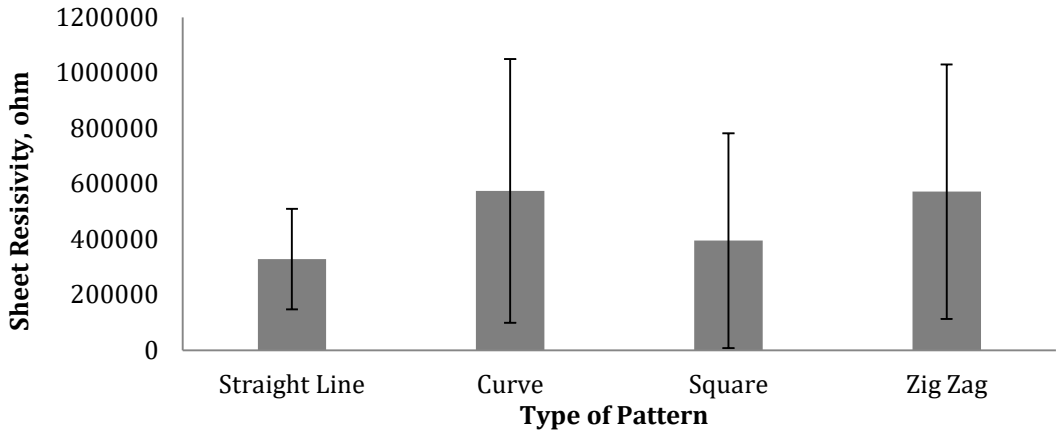

Figure 7. Sheet resistivity at different patterns for 3 mm width.

3.2 Nanoindentation

Figure 8 presents the results of hardness for four patterns of graphene ink samples. Based on the figure, the curve pattern with 3 mm width gives the highest value of hardness and the straight line pattern with 2 mm width gives the lowest value of hardness. In principle, densification of the material generated by crushing under indenter could significantly increase the local elastic modulus. This lack of sensitivity to densification is presumably because the densified zone is small as compared with the longer range of elastic deformation of the rest of the material [21].

Besides that, Figure 9 indicates the results of Young's Modulus of the graphene ink samples for straight-line pattern, curve pattern, square pattern and zig-zag pattern. Based on Figure 9, for the straight-line pattern with 2 mm of width shows the values of elastic modulus less than 3 mm width. The value of 2 mm width is 221.069 GPa and for 3 mm width is 408.714 GPa. The values show that the elastic modulus of 3 mm of width is better than 2 mm width for the straight-line pattern. For the curve pattern, the graph shows increasing values of elastic modulus as compared to the straight-line pattern for both widths. The elastic modulus for curve pattern is better than the straight line. By referring to the square pattern; the elastic modulus value of 2 mm width is higher than 3 mm width for the same pattern but it is still the highest among all the patterns. The value of elastic modulus for 2 mm is 788.383 GPa and for 3 mm is 575.807 GPa. The difference

is about 212.573 GPa. The last pattern in this study is zig-zag. Based on the figure, the values of elastic modulus are 273.405 GPa and 172.375 GPa for 3 mm and 2 mm of width accordingly for the zig-zag pattern. It shows that the elastic modulus for zig-zag is the lowest among the other patterns. As the width of graphene reduces, excess edge energy associated with free edge atoms induces an initial strain on the relaxed configuration of the sheets. This initial strain has a greater influence on Young's modulus of the zig-zag sheet as compared to that of armchair sheets [22].

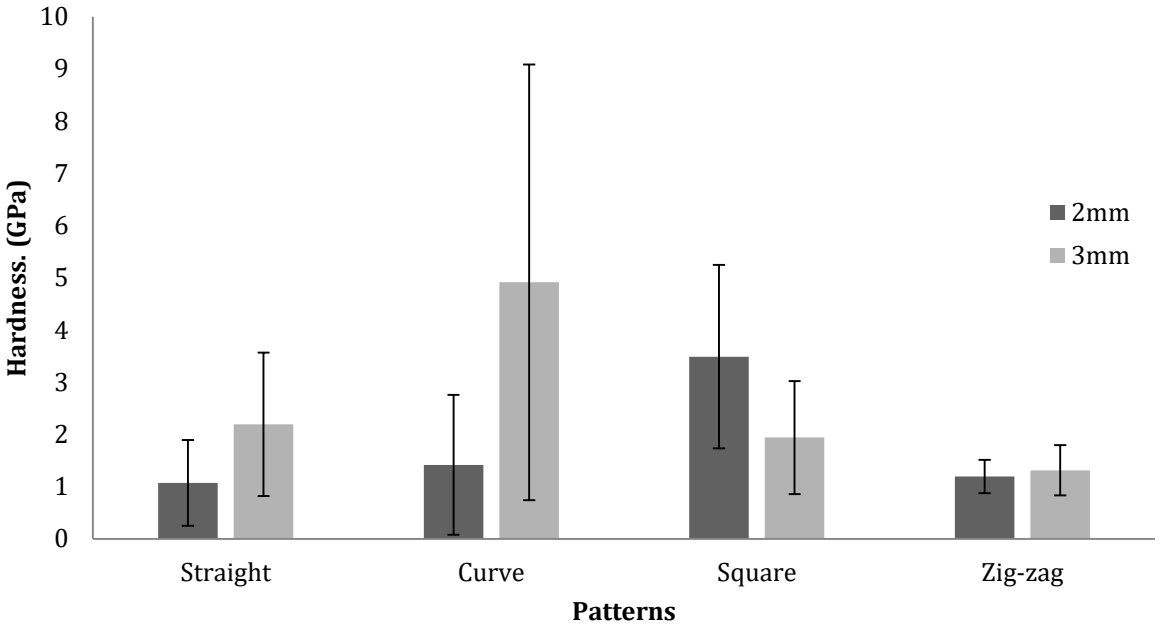

Figure 8. Hardness (GPa) at different patterns.

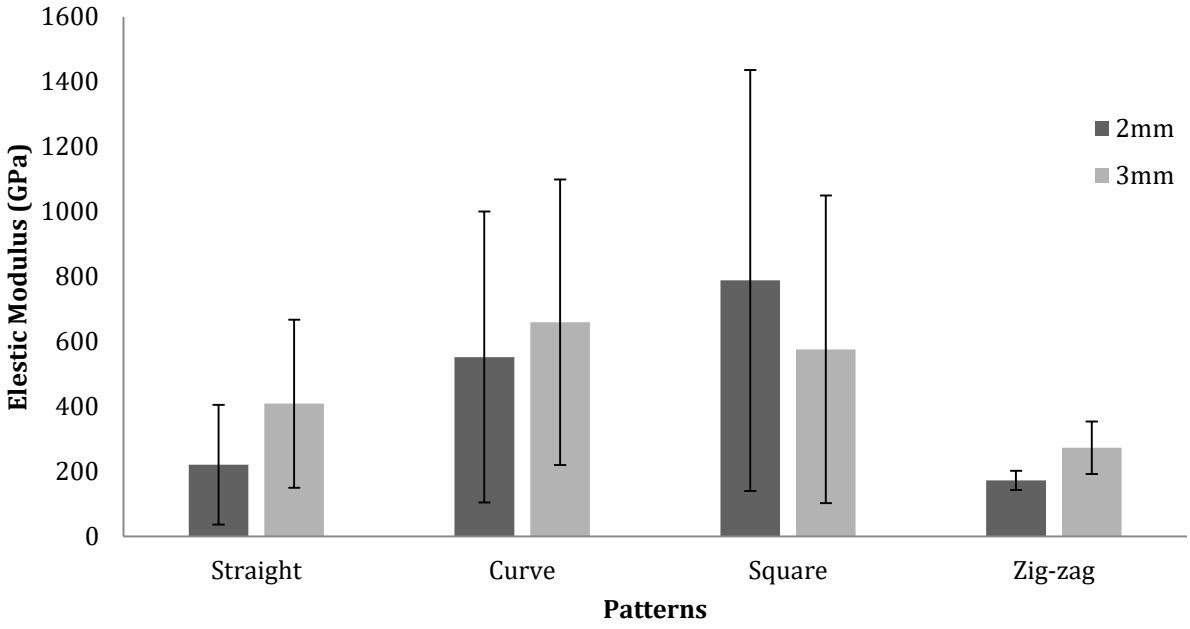

Figure 9. Elastic modulus (GPa) at different patterns.

4. CONCLUSION

Mechanical performance of nanoscale graphene nanoparticles was considered, suitable for electronic component production. Sample preparation and mechanical test setup were briefly described. Nanoindentation tests were performed to see how different parameters, such as different patterns (straight line, curve, square and zig-zag) and width of graphene nanoparticles conductive ink influence the Young's Modulus and hardness of the substrate. According to the average value of indentation of graphene, it was found that the smaller the width, the higher the Young's Modulus values and the biggest the width, the highest the values of hardness. This research provides very useful information about nanoscale graphene nanoparticles of conductive ink based on nanoindentation on flexible substrates for different industrial applications.

ACKNOWLEDGEMENT

The authors gratefully acknowledge to Fakulti Kejuruteraan Mekanikal, Universiti Teknikal Malaysia Melaka (UTeM) for providing laboratory facilities.

REFERENCES

[1] Finkenstadt, V. L., &J. L. Willett. Electroactive materials composed of starch. Journal of Polymers and the Environment, 2 (2004) 43-46.
[2] Alemour, Belal, M. H. Yaacob, H. N. Lim, & Mohd Roshdi Hassan. Review of Electrical Properties of Graphene Conductive Composites. International Journal of Nanoelectronics & Materials, 4 (2018).
[3] Novoselov, Kostya S., Andre K. Geim, Sergei V. Morozov, D. Jiang, Y_ Zhang, Sergey V. Dubonos, Irina V. Grigorieva, & Alexandr A. Firsov. Electric field effect in atomically thin carbon films. Science, 5696 (2004) 666-669.
[4] Balandin, Alexander A., Suchismita Ghosh, Wenzhong Bao, Irene Calizo, Desalegne Teweldebrhan, Feng Miao, & Chun Ning Lau. Superior thermal conductivity of single-layer graphene. Nano Letters, 3 (2008) 902-907.
[5] Novoselov, Kostya S., Andre K. Geim, SVb Morozov, Da Jiang, Michail I. Katsnelson, IVa Grigorieva, SVb Dubonos, & AA Firsov. Two-dimensional gas of massless Dirac fermions in graphene. Nature, 7065 (2005) 197-200.
[6] Zhu, Yanwu, Shanthi Murali, Weiwei Cai, Xuesong Li, Ji Won Suk, Jeffrey R. Potts, & Rodney S. Ruoff. Graphene and graphene oxide: synthesis, properties, and applications. Advanced Materials, 35 (2010) 3906-3924.
[7] Lee, Changgu, Xiaoding Wei, Jeffrey W. Kysar, & James Hone. Measurement of the elastic properties and intrinsic strength of monolayer graphene. Science, 5887 (2008) 385-388.
[8] Verma, Deepak, & Kheng Lim Goh. Functionalized Graphene-Based Nanocomposites for Energy Applications. In Functionalized Graphene Nanocomposites and their Derivatives, Elsevier, (2019) 219-243.
[9] Allen, Matthew J., Vincent C. Tung, & Richard B. Kaner. Honeycomb carbon: A review of graphene. Chemical Reviews, 1 (2010) 132-145.
[10] He, Pei, & Brian Derby. Inkjet printing ultra-large graphene oxide flakes. 2D Materials, 2 (2017) 021021.
[11] Secor, Ethan B., Pradyumna L. Prabhumirashi, Kanan Puntambekar, Michael L. Geier, & Mark C. Hersam. Inkjet printing of high conductivity, flexible graphene patterns. The journal of Physical Chemistry Letters, 8 (2013) 1347-1351.
[12] Su, Yang, Jinhong Du, Dongming Sun, Chang Liu, & Huiming Cheng. Reduced graphene oxide with a highly restored π-conjugated structure for inkjet printing and its use in all-carbon transistors. Nano Research, 11 (2013) 842-852.

[13] Kelly, Adam G., Toby Hallam, Claudia Backes, Andrew Harvey, Amir Sajad Esmaeily, Ian Godwin, João Coelho *et al.* All-printed thin-film transistors from networks of liquid-exfoliated nanosheets. Science, 6333 (2017) 69-73.
[14] Secor, Ethan B., Sooman Lim, Heng Zhang, C. Daniel Frisbie, Lorraine F. Francis, & Mark C. Hersam. Gravure printing of graphene for large-area flexible electronics. Advanced Materials, 26 (2014) 4533-4538.
[15] Arapov, Kirill, Eric Rubingh, Robert Abbel, Jozua Laven, Gijsbertus de With, & Heiner Friedrich. Conductive screen printing inks by gelation of graphene dispersions. Advanced Functional Materials, 4 (2016) 586-593.
[16] Secor, Ethan B., Theodore Z. Gao, Manuel H. Dos Santos, Shay G. Wallace, Karl W. Putz, & Mark C. Hersam. Combustion-assisted photonic annealing of printable graphene inks via exothermic binders. ACS Applied Materials & Interfaces, 35 (2017) 29418-29423.
[17] Gong, Jianghong, Zhijian Peng, & Hezhuo Miao. Analysis of the nanoindentation load–displacement curves measured on high-purity fine-grained alumina. Journal of the European Ceramic Society, 5 (2005) 649-654.
[18] Oliver, Warren Carl, & George Mathews Pharr. An improved technique for determining hardness and elastic modulus using load and displacement sensing indentation experiments. Journal of Materials Research, 6 (1992) 1564-1583.
[19] Vasiljevic, Dragana Z., Aleksandar B. Menicanin, & Ljiljana D. Zivanov. Mechanical characterization of ink-jet printed ag samples on different substrates. In Doctoral Conference on Computing, Electrical and Industrial Systems,. Springer, Berlin, Heidelberg, (2013) 133-141
[20] Saidina, D. S., N. Eawwiboonthanakit, M. Mariatti, S. Fontana, & Claire Hérold. Recent Development of Graphene-Based Ink and Other Conductive Material-Based Inks for Flexible Electronics. Journal of Electronic Materials, 6 (2019) 3428-3450.
[21] Chen, Zhangwei, Xin Wang, Vineet Bhakhri, Finn Giuliani, & Alan Atkinson. Nanoindentation of porous bulk and thin films of La0. 6Sr0. 4Co0. 2Fe0. 8O3− δ. Acta Materialia, 15 (2013) 5720-5734.
[22] Dewapriya, M. A. N., A. Srikantha Phani, & R. K. N. D. Rajapakse. Influence of temperature and free edges on the mechanical properties of graphene. Modelling and Simulation in Materials Science and Engineering, 6 (2013) 065017.